A topological stitching strategy for biocompatible wet adhesion using mussel-inspired polyurethane

Buyun Chen[1], Kun Lei[2], Dandan Zhu[1], Chongchong Yang[1], Chengyuan Sun[1], Wei Xiao[1], Zhen Zheng[1] and Xinling Wang[1*]

[1] *School of Chemistry and Chemical Engineering, State Key Laboratory of Metal Matrix Composites, Shanghai Jiao Tong University, Shanghai 200240, China*

[2] *School of Medical Technology and Engineering, Henan University of Science and Technology, Luoyang 471023, China*

Abstract:

The biomedical and surgical applications of hydrogels demand effective methods to adhere hydrogels to diverse substrates including living tissues. Here we present a mussel mimetic polyurethane as topological suture material for tough adhesion of hydrogels by introducing catechol moieties into polymer chains. Solution of the stitching polyurethane can be injected onto the surface of a hydrogel, followed by diffusing spontaneously into the hydrogel, then get triggered by oxidant for in situ gelation. Oxidative cross-linkage of catechol-modified polyurethane after penetration into hydrogels or living tissues could establish enough covalently entangled networks to afford desired adhesion strength. The mussel mimetic polyurethane demonstrates excellent adhesion strength of hydrogels to universal substrates including inorganics, polymers, and biomaterials, with no requirements for specific functional groups or chemical modification. The adhesion energy achieved by the topological stitching strategy can reach up to 350 J/m^2. Moreover, the stitching polymer shows good biocompatibility and the potential for debonding under the catalysis of elastase. This work will possibly become a promising strategy candidate for adhesion in wet environments.

Key words: Wet adhesion, Topological stitching, Polyurethane, Mussel-inspired,

[*] *Corresponding author at: School of Chemistry and Chemical Engineering, State Key Laboratory of Metal Matrix Composites, Shanghai Jiao Tong University, 800 Dongchuan Road, Shanghai 200240, China. E-mail: xlwang@sjtu.edu.cn*

Catechol chemistry

1 Introduction

Hydrogels adhered to diverse materials grant the substrates hydrophilicity, lubricity and biocompatibility, thus demonstrating infinite potential in emerging fields such as drug delivery [1-4], wound closure [5-8], stretchable bioelectronics [9-15], soft robots [16-19], and marine antifouling [20]. However, establishing an effective adhesion between hydrogels and most substrates is a hard task due to the abundance of water in hydrogels. Disadvantages of typical adhesives include weak bonding strength, poor biocompatibility and inapplicability with wet soft surfaces, limiting the practical application of hydrogels [21]. For example, when the commercial cyanoacrylate glue, which processes an excellent adhesion strength, is applied to a wet and soft surface, it will rapidly form a hard plastic layer and consequently loses the adhesion ability. So far, numerous fundamental works have been carried out on integrating hydrogels with diverse hard or soft substrates [21-23]. Among them, chemical bonding is the most common method to achieve robust adhesion with hydrogels. To illustrate, the double layer hydrogel adhesive with impressive adhesion strength uses a bridging polymer with amino groups to bond with carboxyl groups on the surfaces of hydrogel and biological tissue [5]. However, the strategy of covalent bonding suffers from the limitation of requiring specific functional groups [5, 24], previous chemical modifications [25, 26], complex hierarchical designs [16], or toxic reagents [27]. Therefore, a universal strategy for tough adhesion of hydrogel remains a challenge.

Topological adhesion developed in recent years is a promising strategy combining covalent bonding, interchain interaction and entanglement of polymer network [28-30]. The stitching polymers utilized in topological adhesion are long chain macromolecules containing reactive sites. In a typical process of topological adhesion, precursors of the stitching polymer diffuse into the preformed hydrogel, then get triggered to crosslink mutually and form a network in situ. The stitching network could be constructed by either hydrogen bonds [28], polyelectrolyte complexes [29], or covalent bonds [30]. The gelation of the stitching polymer can be rapid (50 J/m^2 in 60 s) and the resultant adhesion can be quite strong (above 1000 J/m^2) as well [31]. Since the reaction between

the stitching polymer and hydrogel is not a necessity, no specific functional groups on hydrogel or adherend are required. Thereby, theoretically an arbitrary hydrogel could be adhered to all sorts of substrates by means of topological adhesion. The advantageous strength of topological adhesion originates from the synergistic effect of interfacial adhesion, internal cohesion and efficient stress dissipation [21]. However, the topological adhesion has its own limitation. For adherends with a compact structure, the stitching polymer is difficult to penetrate or generate effective entanglements. Thus, the topological stitching strategy needs to be modified.

Polyurethane is a type of unique synthetic polymer with excellent biocompatibility, flexibility and tunable structure [32, 33], and has been widely used as coatings, adhesives, and thermoplastic elastomers. The U.S. Food and Drug administration (FDA) has approved the application of polyurethane as biomaterial owing to its outstanding properties. By alternating the "soft" and "hard" segments in the polymer chain, structure, morphology, and mechanical properties of polyurethane could be easily adjusted for desired performances [34, 35]. Taking advantage of the isocyanate groups in polyurethane, functional groups such as catechol could be efficiently and quantitatively grafted onto designed sites of polymer chain [36-39]. Furthermore, its high cohesive energy is also conducive to the formation of robust topological entanglement with hydrogels and adherends via hydrogen bond, π-π stacking and other interactions.

Catechol moiety plays a crucial role in the tight adhesion of some marine organism to all kinds of surfaces in wet environments [40-44]. Combining mussel adhesive moiety dopamine and bio-functional moiety L-lysine, our group successfully synthesized functional molecule lysine-dopamine (LDA) and used it as chain extender to produce mussel mimetic functional polyurethane [45]. The catechol chemistry enables the adhesion of the catechol modified polyurethane to solid adherends such as glass or steel by chemical bonding. For living tissues which are essentially hydrogels composed of proteins and peptides, the incorporation of lysine-dopamine with similar peptide structure may facilitate the penetration and reinforce the adhesion. Meanwhile, the stitching network can be facilely generated by oxidative polymerization of catechol

triggered by addition of oxidant like sodium periodate. Additionally, the peptide bond in LDA could be identified and cut off easily by corresponding protease, which demonstrates the possibility of debonding between hydrogels and adherends [46].

Herein, we report a topological stitching strategy using mussel mimetic polyurethane as the stitching polymer on basis of our previous work [47]. With a combined function of chemical bonding and topological entanglement, an effective adhesion between random hydrogels and adherends was realized. The mussel mimetic polyurethane can function as a topological suture material for strong adhesion of hydrogel to universal substrates including glass, metal, polymers, and biomaterials, with satisfying adhesion ability, great biocompatibility and potential for biocatalytic debonding. This work is hoped to be a promising alternative for wet adhesion in biomedical and surgical use.

2 Material and Methods

2.1 Materials

Dopamine hydrochloride (DA·HCl, InnoChem), 1,6-hexamethylene diisocyanate (HDI, Aladdin), stannous octoate ($Sn(Oct)_2$, Adamas-Beta), triethylamine (TEA, Adamas-Beta) and anhydrous diethyl ether (Et_2O, General-Reagent) were used as received without further purification. Polyethylene glycol (PEG, M_w= 2000, J&K Scientific) was dried under vacuum at 110 ℃ for 2 h before use. N,N-Dimethylformamide (DMF, Sinopharm Chemical Reagent Co., Ltd.) was refluxed with calcium hydride (CaH_2) for 4 h, distilled under vacuum at 60 ℃, and stored in the presence of 4 Å molecule sieves before use. LDA (Lysine-Dopamine) was synthesized in the laboratory. To prepared the polyacrylamide (PAAm) hydrogel, acrylamide (AAm, Adamas-Beta) was used as monomer, and N,N'-Methylenebisacrylamide (MBAA, Adamas-Beta) was used as crosslinker. 2-Hydroxy-4'-(2-Hydroxyethoxy)-2-Methylpropiophenone (MBAA, Adamas-Beta) was used as free radical initiators for polymerization. Glass, mica, stainless steel, aluminum oxide (Al_2O_3), copper oxide (CuO), polypropylene (PP), expanded polystyrene (EPS), polyethylene terephthalate (PET), polyvinyl chloride (PVC), polymethylmethacrylate (PMMA), polytetrafluoroethylene (PTFE), bovine bone, porcine skin and liver were used as

representative adherends and obtained from commercial market. The surface of the adherends were cleaned with ethanol and dried before experiment. Elastase (30 units/mg, Shanghai Yuanye Bio-Technology Co., Ltd) was used in the biodegradation test. Dulbecco's modified eagle medium (DMEM, Gibco) and fetal bovine serum (FBS, Corning) were used in cytotoxicity test.

2.2 Preparation of glue polymer solution

Synthesis of mussel-mimetic polyurethane (PU-LDA): The mussel-mimetic polyurethane (PU-LDA) was synthesized from HDI, PEG and chain extender LDA using a multistep solution polymerization in DMF according to our previous work [47]. To a solution of polyethylene glycol (PEG, M_w= 2000, 1 equiv.) in DMF were added 1,6-hexamethylene diisocyanate (HDI, 2 equiv.) and 2 drops of $Sn(Oct)_2$ (catalyst) under a dry nitrogen atmosphere at 70 ℃. After mechanical stirring for 2 h, the prepolymer was cooled to 0 ℃, and chain extender LDA (1.1 equiv.) dissolved in DMF was added. TEA was injected dropwise into the solution to neutralize the hydrochloric acid. After stirring for another 16 h, the reaction mixture was filtrated, precipitated in anhydrous diethyl ether, dialyzed and lyophilized to afford desired product PU-LDA as white powder. GPC found M_n = 18233, M_w = 24793, PDI = 1.360.

Preparation of the stitching polymer PU-LDA solution: PU-LDA (1.31 g) was dissolved in 10 mL deionized water. DA·HCl (95 mg, 0.5 mmol) was added and the final concentration of catechol was 100 mM. The pH of the glue polymer solution was tested to be 7.5 (Mettler Toledo pH meter, FE20).

2.3 Measurements

Nuclear magnetic resonance (NMR) spectroscopy: The NMR spectra of synthesized LDA and LDA containing polyurethane (PU-LDA) were measured with a Bruker (AVANCE III HD 500, 500 MHz) NMR spectrometer at room temperature. Dimethyl sulfoxide-d_6 was used as the solvent.

FT-IR spectroscopy: The FT-IR spectra of LDA and PU-LDA were measured with a Perkin-Elmer (Spectrum 1000) FT-IR spectrometer at room temperature. Powdered samples were studied (KBr pellets).

UV-vis spectroscopy: The UV-vis spectra of LDA and PU-LDA were measured

with a Perkin-Elmer (Lambda 35) UV-vis spectrometer at room temperature using H_2O as solvent. All measurements were performed in quartz cuvettes. The scan range was 200-800 nm, and the scan rate was 960 nm/min.

Quadrupole time-of-flight mass spectroscopy (QTOF-MS): The mass spectrum of LDA was measured with a Bruker (Bruker impact II) QTOF mass spectrometer. Methanol is used as the solvent and the concentration of LDA is 0.05 mg/mL.

Thermogravimetry analysis (TGA): Thermal decomposition of PU-LDA was tested with a TA (Discovery TGA550) thermogravimetric analyzer under a nitrogen flow (100 mL/min) from 50 to 600 °C at a heating rate of 20 °C/min.

Differential scanning calorimetry (DSC): Thermal property of PU-LDA was tested with a TA (Q2000) modulated differential scanning calorimetry. The DSC cell was purged with a stream of 50 mL/min nitrogen. The weight of the sample was 10 mg. The following the procedure was performed: the sample was first heated to 200 ℃ at a rate of 20 ℃/min, then cooled to -60 ℃ at a rate of 10 ℃/min, and finally heated to 200 ℃ at a rate of 10 ℃/min.

Peeling test for measuring adhesion energy: 90-degree peeling test was conducted to measure the adhesion energy of the peeling samples using a universal testing machine (Model 43 MTS Criterion) with a 500 N load cell. The peeling samples were 75 mm long, 15 mm wide, and 2 mm thick. The back side of the hydrogel was glued to an inextensible, 20-μm-thick polyester film using cyanoacrylate (Krazy glue). The free end of the backing layer was fixed to the tensile tester and peeled at a rate of 0.5 mm/s. Rigid adherend was fixed horizontally, and soft adherend was glued to a piece of glass with Krazy glue prior to the test. The force was measured as a function of displacement. The adhesion energy was calculated the plateau value of the peeling force divided by the width of the hydrogel. The tests were repeated at least 3 times and the averages with standard deviations were reported.

Biocatalytic debonding test: 90-degree peeling samples prepared via stitching strategy were immersed in a solution of PBS (0.01 M, pH = 7.4) containing elastase (30 units/mL) for 12, 24, 36, 48 h at 25 ℃. For experiments more than 24 h, PBS was refreshed to keep the activity of the enzyme. Samples incubated in PBS without the

enzyme at 37 ℃ were set as controls. The adhesion energy of the samples was measured by 90-degree peeling test. The tests were repeated at least 3 times and the averages with standard deviations were reported.

Cell viability assay: According to MTT cytotoxicity assay, in *vitro* cytocompatibility of PU-LDA lyophilized powder and the extracts of the PU-LDA hydrogel formed by oxidative crosslinking was evaluated utilizing HeLa cells. Typically, HeLa cells were seeded into 96-well plates at a density of 10^4 cells per well and cultured in Dulbecco's modified Eagle medium (DMEM) containing 10% fetal bovine serum (FBS) at 37 ℃ in a humidified atmosphere containing 5% CO_2 to obtain a monolayer of cells. Hydrogel extracts were acquired by adding 1 g PU-LDA hydrogel fragments to 10 mL DMEM, soaked at 37 ℃ for 24 h, and diluted 10, 100, 1000 times with DMEM. Subsequently, culture medium was replaced by the gel extracts at different concentrations and further incubated for 24 or 72 h. The cells cultured in the pure DMEM were set as the control. The sample solution was removed after incubation and the cells were further cultured with 50 μL of MTT solution (1 mg/mL) for 4h. Finally, the culture medium was substituted with 150 μL of DMSO and the absorbance of the DMSO solution at 490 nm was tested by a microplate reader (Tecan, Infinite M1000 Pro). The relative cell viability was calculated the mean absorbance value of the sample divided by that of the control. The assay was performed 6 times for each culture and the averages with standard deviations were reported. The sample with relative cell viability more than 70% was considered to be biocompatible. The in *vitro* cell viability assay of PU-LDA lyophilized powder with the concentrations of 10 mg/mL and 1mg/mL was conducted using similar method as shown above.

3 Results and discussion

3.1 Synthesis of mussel mimetic polyurethane for the topological stitching strategy

The mussel mimetic polyurethane PU-LDA was synthesized from HDI, PEG and chain extender LDA in accordance to our previous work [47] (Supporting Information, Scheme S1). NMR, FTIR, and other analytical measurements were conducted to characterize LDA and PU-LDA (Fig. S1-S9).

The stitching polymer PU-LDA solution consisted of two major components:

catechol containing long-chain polyurethane as framework, and dopamine as crosslinking units. As illustrated in Fig. 1a, in a representative procedure of stitching strategy, the stitching polymer solution was injected onto the surface of a hydrogel and penetrated into the hydrogel network. Then the oxidant, sodium periodate ($NaIO_4$) solution was added to the surface of the hydrogel, followed by pressing the adherend on top and compressing at a constant strain. After mixing with $NaIO_4$, catechol units in the stitching polymer solution started to be oxidized almost immediately, and the assembly turned orange within a few seconds. Dopamine diffused through the hydrogel network easier than the polyurethane and acted as crosslinking points inside the gel (Fig. 1b). Based on literature [47], multiple mechanisms can explain oxidative crosslinking of catechol, including oxidative coupling of catechol, formation of imide by Schiff-base reaction between dopamine and quinone, coupling between dopamine and quinone by Michael-addition reaction, etc. Non-covalent intermolecular interactions such as π-π stacking and hydrogen bond between carbamate and catechol also participated in the formation of crosslinked network in the stitching polymer solution (Fig. 1c). After complete gelation, the covalent network built by oxidative crosslinking of catechol entangled with the hydrogel network, thus to realize the stitching target.

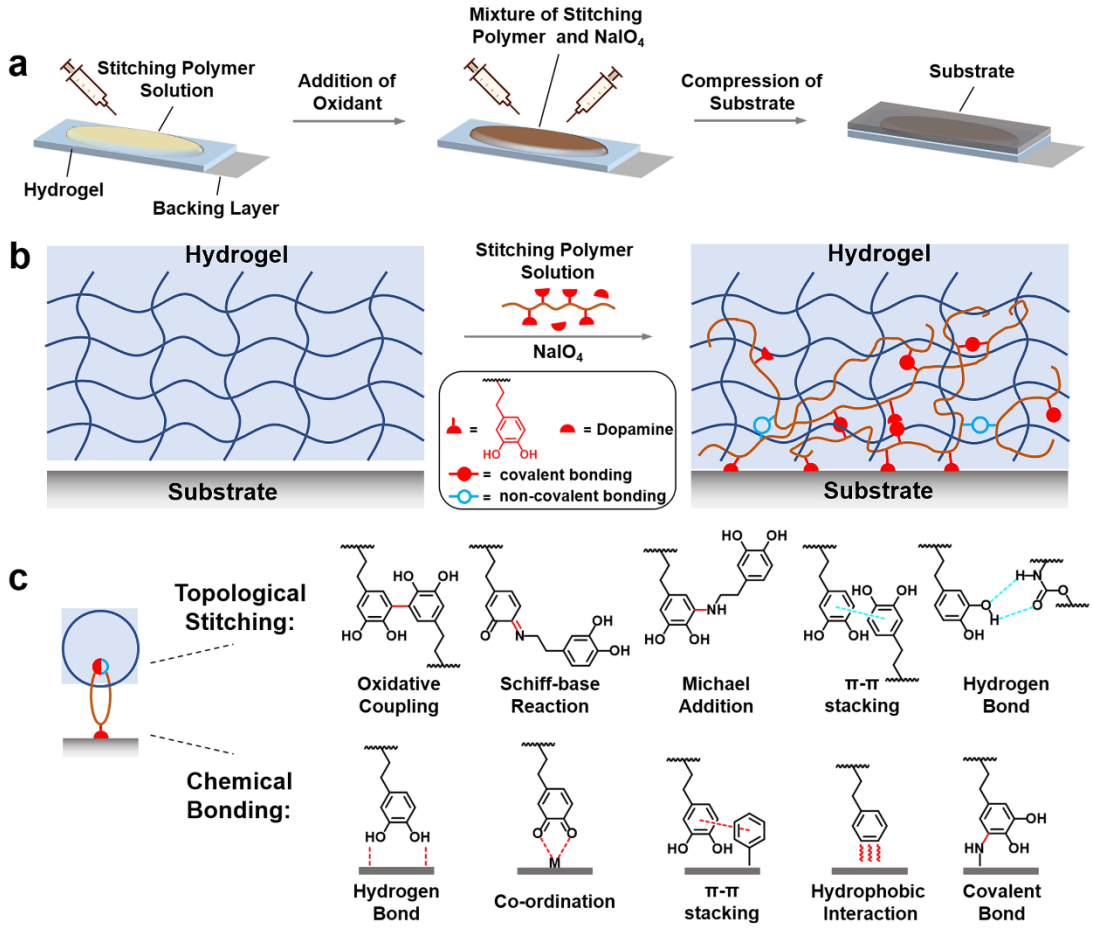

Fig. 1. Principle of the topological stitching strategy. a) Schematic of experimental procedure of the stitching strategy. b) Mechanism of the topological stitching strategy. c) Representative interactions in topological stitching and chemical bonding.

3.2 Universal adhesion of diverse substrates

A universal stitching strategy retains good adhesion strength for varied texture of adherends. PAAm hydrogel, consisted of covalent crosslinked networks with no reactive functional group, was utilized as the model hydrogel. A series of adherends were tested to evaluate the versatility of the stitching polymer PU-LDA solution, including glass, mica, stainless steel, aluminum oxide (Al_2O_3), copper oxide (CuO), polypropylene (PP), expanded polystyrene (EPS), polyethylene terephthalate (PET), polyvinyl chloride (PVC), polymethylmethacrylate (PMMA), polytetrafluoroethylene (PTFE), bovine bone, porcine skin and liver. As presented in Fig. 1c, the catechol containing stitching polymer can adhere to different surfaces via various interactions: hydrogen bond with inorganic silicate, coordination with metal ion, π-π stacking or

hydrophobic interaction with polymer containing benzene ring or long alkane chain, covalent bonding with amino group on living tissue, etc. The hydrogel and the adherend were topologically stitched together via oxidative crosslinking of the stitching polymer solution, then 90-degree peeling test was conducted to measure the adhesion energy between them. Photographs of representative adherends showed obvious cohesive peeling front and brush-hair pattern for glass, stainless steel and PMMA (Fig. 2b). Deformation of hydrogel and entanglement with the adherend surface for porcine skin were observed as well, which represented the strength of the topological stitching. For all non-biological materials except PTFE, tough adhesion was achieved with adhesion energy over 200 J/m^2, which is approximately the fracture toughness of the PAAm hydrogel and tough living tissue (Fig. 2c) [48]. Adherends of top three adhesion strength were glass, CuO and PMMA, with adhesion strength of 353.1, 326.3 and 321.8 J/m^2, respectively. The excellence of these adherends was likely to result from the strong interaction of hydrogen bond or coordination between the stitching polymer and the adherends. For biological materials, the adhesion strength decreased slightly but still remained at a relative high level with cohesive adhesion (around 150 J/m^2). Hence, the stitching strategy based on catechol chemistry was proved to be applicant for universal adhesion.

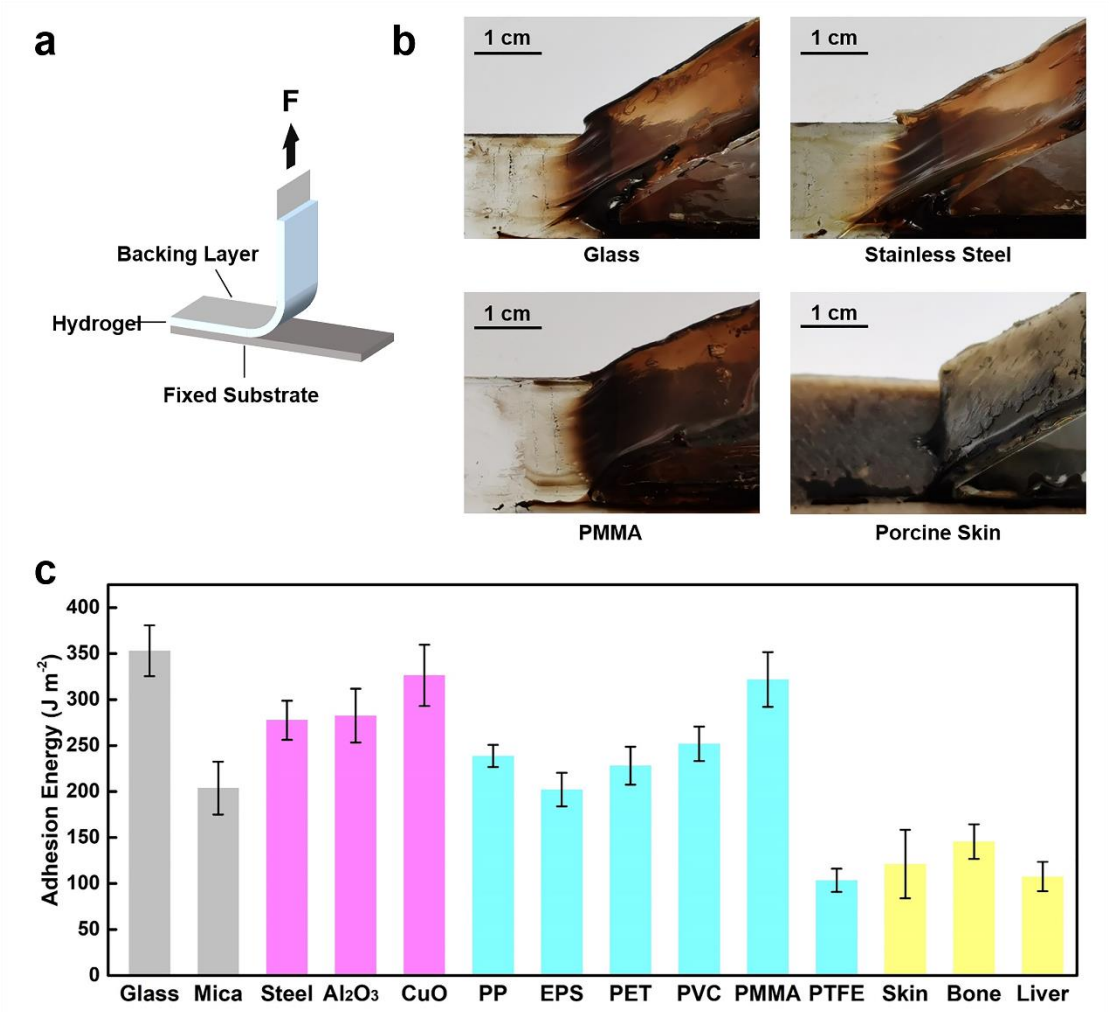

Fig. 2. Versatility of adhesion to diverse substrates using PU-LDA. a) Schematic of 90-degree peeling test. b) Experimental photographs of four representative adherends. c) Adhesion energies of PAAm hydrogel to 14 different adherends.

3.3 Mechanism of the topological adhesion

A thorough understanding of mechanism is essential for methodology development of topological stitching, therefore investigation of the chemistry behind the robust adhesion was conducted. PAAm hydrogel and glass were chosen as the representative hydrogel and adherend, respectively. The adhesion energy was measured by 90-degree peeling test.

The stitching condition was optimized by varying the component of the stitching polymer solution and the concentration of $NaIO_4$. Stitching solutions with different molar ratios of PU-LDA and dopamine were prepared, and the concentration of catechol

was fixed at 100 mM. As the content of dopamine increased, the adhesion strength first raised, and then dropped significantly (Fig. 3a). The maximum was 353.1 J/m^2 at the molar ratio of dopamine/catechol being 50% in the stitching solution. The addition of dopamine densified the entanglement within the PAAm network, thus made for tough adhesion. However, excess dopamine declined the amount of PU-LDA which acted as the backbone of the stitching polymer, and consequently reduced the mechanical strength after gelation, therefore causing poor performance in the peeling. Subsequently, the ratio of dopamine/catechol was fixed at 50%, and the influence of ratios of $NaIO_4$/catechol were further investigated. As the concentration of $NaIO_4$ increased, more crosslinking points were formed via the oxidation of catechol (Fig. 3b). When molar amount of $NaIO_4$ was less than catechol, the adhesion strength increased with the addition of $NaIO_4$. Yet, with too much addition of $NaIO_4$, the bidentate hydroxyl on catechol was oxidized to *o*-quinone, which lost the ability to form covalent crosslink or hydrogen bond, therefore resulting in a weak adhesion.

The kinetics of the stitching process was investigated detailedly by measuring the correlation between adhesion energy and pH of the stitching polymer solution, penetration time, and adhesion time. According to literature, alkaline environment could influence the crosslinking of the catechol by accelerating the oxidation process. Stitching polymer solutions were prepared using buffer solutions of different pH values. In neutral or slightly alkaline environment, tough adhesion was achieved (over 250 J/m^2) (Fig. 3c). The result showed the stitching strategy was applicable for daily or biomedical use. The adhesion strength dropped in acidic environment as acid could retard the oxidative crosslinking of catechol. On the contrast, in a strong alkaline environment, the oxidative crosslinking proceeded so fast that few catechol was able to penetrate into the gel, thus not enough entanglements were formed to afford a tough adhesion. Stitching polymers penetrated into the hydrogel immediately after being added to the surface. To evaluate the speed of the penetration process, the adhesion energy was measured as a function of the penetration time. After a short time (1 min or 2 min), the adhesion strength reached over 300 J/m^2 (Fig. 3d), indicating the stitching polymer penetrated at a rather fast speed. For penetration over 30 min, the differential

mobility of dopamine led to reduced catechol concentration on the adherend surface and fewer crosslinked networks, and consequently decreased adhesion strength. Adhesion time was also tested. The adhesion energy increases with the adhesion time until a plateau was reached after 12h (Fig. S10).

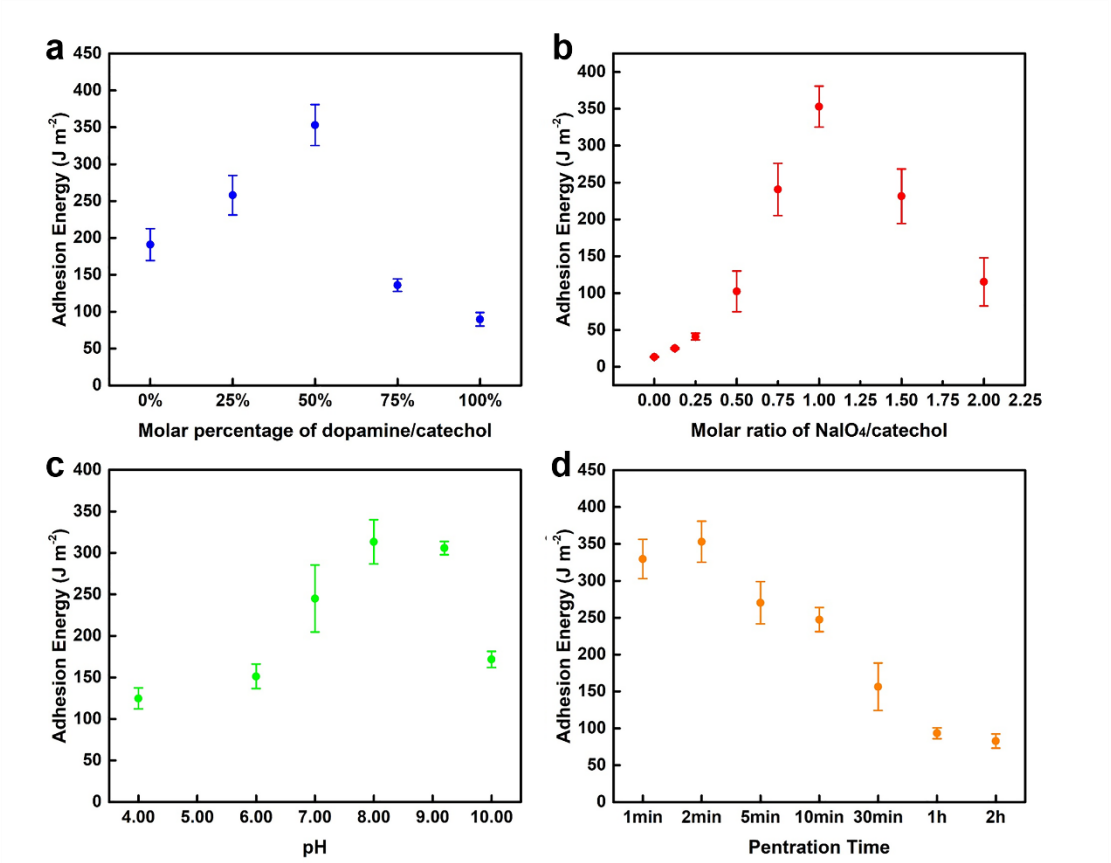

Fig. 3. Adhesion energy as a function of several variables. In a representative procedure, 400 μL stitching polymer solution (c[catechol] = 100 mM) was added to the surface of PAAm hydrogel. After penetrating for 2 min, the stitching polymer solution was mixed evenly with 100 μL $NaIO_4$ (400 mM) as oxidant. The glass was pressed on the top and the assembly was compressed at a constant strain of ~5 % for 12 h. Each variable was investigated with others fixed. a) Adhesion energy as a function of molar percentage of dopamine/catechol. b) Adhesion energy as a function of molar ratio of $NaIO_4$/catechol. c) Adhesion energy as a function of pH. d) Adhesion energy as a function of penetration time.

3.4 Function of the topological stitching strategy

The adhesion energy of topological stitching consisted of two components: the entanglement between covalent networks, and the non-covalent interactions including

hydrogen bond, etc. Since covalent bonds are normally stronger than non-covalent interactions in bond energy, the covalent entanglement was assumed as the major contributor of the adhesion strength. The function of the stitching strategy was evaluated by the comparison with non-stitching strategy. In a typical procedure of stitching strategy, the stitching polymer solution and $NaIO_4$ were successively added to the surface of a PAAm hydrogel followed by pressing of the adherend. For non-stitching strategy, the stitching polymer solution and $NaIO_4$ were simultaneously added to the surface of the adherend. After complete gelation, the stitching polymer became immobilized in the crosslinked network, thus losing capability of penetration. The hydrogel was pressed afterwards to avoid covalent entanglements (Fig. 4a, 4b). Four representative adherends (glass, stainless steel, PMMA and porcine skin) were tested with both strategies. The adhesion made by stitching strategy could be quite tough (over 150 J/m^2), contrast to the poor adhesion strength of non-stitching strategy (around 20 J/m^2) (Fig. 4c). The comparison of the results confirmed our hypothesis and validated the formation of covalent entanglement by oxidative crosslinking of catechol. The outcome was also consistent with our previous work, in which mixing polyurethane without catechol moieties and $NaIO_4$ led to no gelation [47].

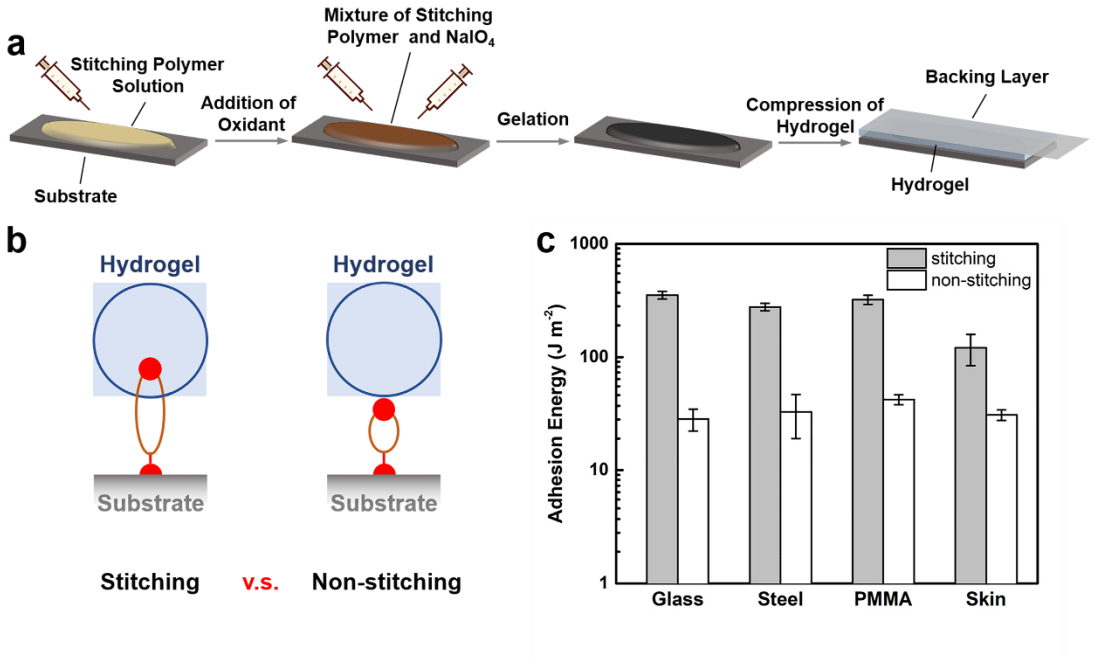

Fig. 4. Effect of the topological stitching strategy on the adhesion energy. a) Schematic of experimental procedure of the non-stitching strategy. b) Comparison of the different topologies of

connection. c) Adhesion energy of four representative adherends by both strategies.

3.5 Performance of biocatalytic debonding and biocompatibility

Biocatalytic debonding and cytocompatibility of the stitching polymer are crucial to biomedical applicability. Owing to the peptide bond in the chain extender LDA granted the stitching polymer biodegradability, elastase was employed to evaluate the biocatalytic debonding of the stitching polymer. The peeling samples were first prepared via stitching strategy, then immersed in a solution of phosphate buffer saline (PBS) containing elastase for 12, 24, 36 and 48 h. Samples incubated in PBS without enzyme were set as controls. After hours of immersion, the adhesion strength of the control remained above 150 J/m^2, presenting good durability of the stitching polymer in aqueous environment (Fig. 5a). Compared to the control, the adhesion strength of sample immersed in elastase solution dropped about 25% at 48 h, indicating fine biocatalytic debonding of the stitching polymer.

In *vitro* cytocompatibility of the stitching polymer prepared by bio-sourced lysine and dopamine, and nontoxic polyurethane was evaluated via MTT assay. Lyophilized powder of PU-LDA and extracts of PU-LDA hydrogel formed by oxidative crosslinking were tested. Both materials showed satisfactory cytocompatibility, with the cell viability over 80% after 24 or even 72 h at different concentration gradients (Fig. 5b, Fig. S11), which illustrated the stitching polymer was capable of biomedical use.

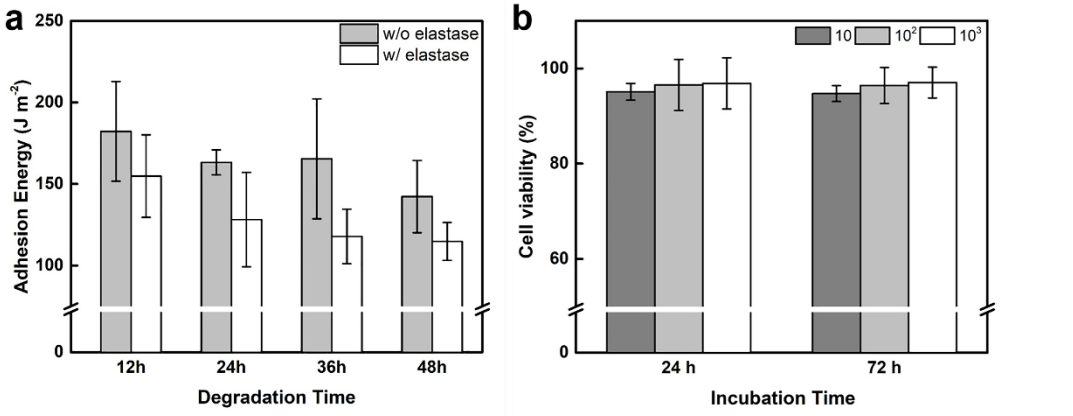

Fig. 5. a) Adhesion energy of four representative adherends as a function of degradation time. b) Cell viability of PU-LDA hydrogel extracts at three different concentration gradients after incubated for 24 or 72 h.

4 Conclusions

In summary, we successfully developed a method of topological adhesion for biocompatible wet adhesion using mussel-mimetic polyurethane. The mussel-mimetic polyurethane demonstrated excellent adhesion strength of hydrogels to universal substrates including inorganics, polymers, and biomaterials, with no requirements for specific functional groups or chemical modification, paving a way for the application of hydrogel adhesive in previously inaccessible conditions. The key of the stitching strategy is to use catechol-modified suture, which could either stitch hydrogels by forming topological entanglements with the hydrogel networks, or bond to the substrate directly by catechol chemistry, Additionally, the stitching polymer demonstrated excellent biocompatibility and the potential for elastase-catalyzed interfacial debonding. The topological stitching strategy is hoped to be employed in biomedical and surgical applications such as drug delivery, wound closure, bioelectronics, etc.

Appendix A. Supplementary data

Supplementary materials include: synthesis steps of lysine-dopamine (LDA); scheme of synthetic procedure of LDA (Sc. S1); preparation of LDA containing polyurethane (PU-LDA) hydrogel and polyacrylamide (PAAm) hydrogel; rheology analysis of PU-LDA hydrogel; experimental procedure of stitching strategy and non-stitching strategy; ^{1}H- and ^{13}C-NMR spectra of LDA and PU-LDA (Fig. S1-S4); FT-IR spectra of LDA and PU-LDA (Fig. S5); UV-vis spectra of LDA and PU-LDA (Fig. S6); TGA and DSC curves of PU-LDA (Fig. S7, S8); dynamic frequency sweep and strain sweep of the PU-LDA hydrogel (Fig. S9); adhesion energy as a function of penetration time (Fig. S10); cell viability of PU-LDA lyophilized powder (Fig. S11).

Declaration of Competing Interest

The authors declare that they have no known competing financial interests or personal relationships that could have appeared to influence the work reported in this paper.

Acknowledgements

This study was financially supported by National Nature Science Foundation of China (22075177). We thank Mr. Xinyang Zhao and Prof. Wei Yu for helping with rheology analysis; Ms. Juan Li, Prof. Xiangyi Huang and Prof. Jicun Ren for helping with cell

viability assay.

Reference

[1] B. Mirani, E. Pagan, B. Currie, M.A. Siddiqui, R. Hosseinzadeh, P. Mostafalu, Y.S. Zhang, A. Ghahary, M. Akbari, An advanced multifunctional hydrogel-based dressing for wound monitoring and drug delivery, Adv. Healthc. Mater. 6 (2017) 1–15. https://doi.org/10.1002/adhm.201700718.

[2] J. Li, D.J. Mooney, Designing hydrogels for controlled drug delivery, Nat. Rev. Mater. 1 (2016) 1–17. https://doi.org/10.1038/natrevmats.2016.71.

[3] Z. Wei, J.H. Yang, Z.Q. Liu, F. Xu, J.X. Zhou, M. Zrínyi, Y. Osada, Y.M. Chen, Novel biocompatible polysaccharide-based self-healing hydrogel, Adv. Funct. Mater. 25 (2015) 1352–1359. https://doi.org/10.1002/adfm.201401502.

[4] S. Banerjee, P. Chattopadhyay, A. Ghosh, P. Datta, V. Veer, Aspect of adhesives in transdermal drug delivery systems, Int. J. Adhes. Adhes. 50 (2014) 70–84. https://doi.org/10.1016/j.ijadhadh.2014.01.001.

[5] J. Li, A.D. Celiz, J. Yang, Q. Yang, I. Wamala, W. Whyte, B.R. Seo, N. V. Vasilyev, J.J. Vlassak, Z. Suo, D.J. Mooney, Tough adhesives for diverse wet surfaces, Science. 357 (2017) 378–381. https://doi.org/10.1126/science.aah6362.

[6] C. Ghobril, M.W. Grinstaff, The chemistry and engineering of polymeric hydrogel adhesives for wound closure: A tutorial, Chem. Soc. Rev. 44 (2015) 1820–1835. https://doi.org/10.1039/c4cs00332b.

[7] P.J.M. Bouten, M. Zonjee, J. Bender, S.T.K. Yauw, H. Van Goor, J.C.M. Van Hest, R. Hoogenboom, The chemistry of tissue adhesive materials, Prog. Polym. Sci. 39 (2014) 1375–1405. https://doi.org/10.1016/j.progpolymsci.2014.02.001.

[8] C. Ghobril, K. Charoen, E.K. Rodriguez, A. Nazarian, M.W. Grinstaff, A dendritic thioester hydrogel based on thiol-thioester exchange as a dissolvable sealant system for wound closure, Angew. Chem. Int. Ed. 52 (2013) 14070–14074. https://doi.org/10.1002/anie.201308007.

[9] W. Li, X. Liu, Z. Deng, Y. Chen, Q. Yu, W. Tang, T.L. Sun, Y.S. Zhang, K. Yue, Tough bonding, on-demand debonding, and facile rebonding between hydrogels and diverse metal surfaces, Adv. Mater. 31 (2019) 1–8. https://doi.org/10.1002/adma.201904732.

[10] Y.J. Hong, H. Jeong, K.W. Cho, N. Lu, D.H. Kim, Wearable and implantable devices for cardiovascular healthcare: from monitoring to therapy based on flexible and stretchable

electronics, Adv. Funct. Mater. 29 (2019) 1–26. https://doi.org/10.1002/adfm.201808247.

[11] C. Yang, Z. Suo, Hydrogel ionotronics, Nat. Rev. Mater. 3 (2018) 125–142. https://doi.org/10.1038/s41578-018-0018-7.

[12] X. Liu, T.C. Tang, E. Tham, H. Yuk, S. Lin, T.K. Lu, X. Zhao, Stretchable living materials and devices with hydrogel-elastomer hybrids hosting programmed cells, Proc. Natl. Acad. Sci. U. S. A. 114 (2017) 2200–2205. https://doi.org/10.1073/pnas.1618307114.

[13] C.C. Kim, H.H. Lee, K.H. Oh, J.Y. Sun, Highly stretchable, transparent ionic touch panel, Science. 353 (2016) 682–687. https://doi.org/10.1126/science.aaf8810.

[14] I.R. Minev, P. Musienko, A. Hirsch, Q. Barraud, N. Wenger, E.M. Moraud, J. Gandar, M. Capogrosso, T. Milekovic, L. Asboth, R.F. Torres, N. Vachicouras, Q. Liu, N. Pavlova, S. Duis, A. Larmagnac, J. Vörös, S. Micera, Z. Suo, G. Courtine, S.P. Lacour, Electronic dura mater for long-term multimodal neural interfaces, Science. 347 (2015) 159–163. https://doi.org/10.1126/science.1260318.

[15] C. Keplinger, J. Sun, C.C. Foo, P. Rothemund, G.M. Whitesides, Z. Suo, Stretchable, transparent, ionic conductors, Science. 341 (2013) 984–988. https://doi.org/10.1126/science.1240228.

[16] H. Yang, C. Li, M. Yang, Y. Pan, Q. Yin, J. Tang, H.J. Qi, Z. Suo, Printing hydrogels and elastomers in arbitrary sequence with strong adhesion, Adv. Funct. Mater. 29 (2019) 1–8. https://doi.org/10.1002/adfm.201901721.

[17] S.I. Rich, R.J. Wood, C. Majidi, Untethered soft robotics, Nat. Electron. 1 (2018) 102–112. https://doi.org/10.1038/s41928-018-0024-1.

[18] H. Yuk, S. Lin, C. Ma, M. Takaffoli, N.X. Fang, X. Zhao, Hydraulic hydrogel actuators and robots optically and sonically camouflaged in water, Nat. Commun. 8 (2017) 1–12. https://doi.org/10.1038/ncomms14230.

[19] T. Li, G. Li, Y. Liang, T. Cheng, J. Dai, X. Yang, B. Liu, Z. Zeng, Z. Huang, Y. Luo, T. Xie, W. Yang, Fast-moving soft electronic fish, Sci. Adv. 3 (2017) 1–8. https://doi.org/10.1126/sciadv.1602045.

[20] X. Yao, J. Liu, C. Yang, X. Yang, J. Wei, Y. Xia, X. Gong, Z. Suo, Hydrogel paint, Adv. Mater. 31 (2019) 1–8. https://doi.org/10.1002/adma.201903062.

[21] J. Yang, R. Bai, B. Chen, Z. Suo, Hydrogel adhesion: a supramolecular synergy of chemistry,

449 topology, and mechanics, Adv. Funct. Mater. 30 (2020) 1–27.
450 https://doi.org/10.1002/adfm.201901693.
451 [22] N. Annabi, A. Tamayol, J.A. Uquillas, M. Akbari, L.E. Bertassoni, C. Cha, G. Camci-Unal,
452 M.R. Dokmeci, N.A. Peppas, A. Khademhosseini, 25th anniversary article: Rational design and
453 applications of hydrogels in regenerative medicine, Adv. Mater. 26 (2014) 85–124.
454 https://doi.org/10.1002/adma.201303233.
455 [23] D.Y. Ko, U.P. Shinde, B. Yeon, B. Jeong, Recent progress of in situ formed gels for
456 biomedical applications, Prog. Polym. Sci. 38 (2013) 672–701.
457 https://doi.org/10.1016/j.progpolymsci.2012.08.002.
458 [24] C.K. Roy, H.L. Guo, T.L. Sun, A. Bin Ihsan, T. Kurokawa, M. Takahata, T. Nonoyama, T.
459 Nakajima, J.P. Gong, Self-adjustable adhesion of polyampholyte hydrogels, Adv. Mater. 27 (2015)
460 7344–7348. https://doi.org/10.1002/adma.201504059.
461 [25] Q. Liu, G. Nian, C. Yang, S. Qu, Z. Suo, Bonding dissimilar polymer networks in various
462 manufacturing processes, Nat. Commun. 9 (2018) 1–11.
463 https://doi.org/10.1038/s41467-018-03269-x.
464 [26] H. Yuk, T. Zhang, G.A. Parada, X. Liu, X. Zhao, Skin-inspired hydrogel-elastomer hybrids
465 with robust interfaces and functional microstructures, Nat. Commun. 7 (2016) 1–11.
466 https://doi.org/10.1038/ncomms12028.
467 [27] D. Wirthl, R. Pichler, M. Drack, G. Kettlguber, R. Moser, R. Gerstmayr, F. Hartmann, E.
468 Bradt, R. Kaltseis, C.M. Siket, S.E. Schausberger, S. Hild, S. Bauer, M. Kaltenbrunner, Instant
469 tough bonding of hydrogels for soft machines and electronics, Sci. Adv. 3 (2017) 1–10.
470 https://doi.org/10.1126/sciadv.1700053.
471 [28] J. Yang, R. Bai, Z. Suo, Topological adhesion of wet materials, Adv. Mater. 30 (2018) 1–7.
472 https://doi.org/10.1002/adma.201800671.
473 [29] Y. Gao, K. Wu, Z. Suo, Photodetachable adhesion, Adv. Mater. 31 (2019) 1–7.
474 https://doi.org/10.1002/adma.201806948.
475 [30] J. Steck, J. Yang, Z. Suo, Covalent topological adhesion, ACS Macro Lett. 8 (2019) 754–758.
476 https://doi.org/10.1021/acsmacrolett.9b00325.
477 [31] J. Steck, J. Kim, J. Yang, S. Hassan, Z. Suo, Topological adhesion. I. Rapid and strong
478 topohesives, Extrem. Mech. Lett. 39 (2020) 100803. https://doi.org/10.1016/j.eml.2020.100803.

[32] J.O. Akindoyo, M.D.H. Beg, S. Ghazali, M.R. Islam, N. Jeyaratnam, A.R. Yuvaraj, Polyurethane types, synthesis and applications-a review, RSC Adv. 6 (2016) 114453–114482. https://doi.org/10.1039/c6ra14525f.

[33] N. Polyurethane, E. Delebecq, J. Pascault, B. Boutevin, U. De Lyon, On the versatility of urethane / urea bonds : reversibility , blocked isocyanate, and non-isocyanate polyurethane, Chem. Rev. 113 (2013) 80–118. https://doi.org/10.1021/cr300195n.

[34] K. Lei, Q. Zhu, X. Wang, H. Xiao, Z. Zheng, In *vitro* and in *vivo* characterization of a foam-like polyurethane bone adhesive for promoting bone tissue growth, ACS Biomater. Sci. Eng. 5 (2019) 5489–5497. https://doi.org/10.1021/acsbiomaterials.9b00918.

[35] P. Du, X. Liu, Z. Zheng, X. Wang, T. Joncheray, Y. Zhang, Synthesis and characterization of linear self-healing polyurethane based on thermally reversible Diels-Alder reaction, RSC Adv. 3 (2013) 15475–15482. https://doi.org/10.1039/c3ra42278j.

[36] E.M. Briz-López, R. Navarro, H. Martínez-Hernández, L. Téllez-Jurado, Á. Marcos-Fernández, Design and synthesis of bio-inspired polyurethane films with high performance, Polymers (Basel). 12 (2020) 1–17. https://doi.org/10.3390/polym12112727.

[37] S. Cao, S. Li, M. Li, L. Xu, H. Ding, J. Xia, M. Zhang, K. Huang, The thermal self-healing properties of phenolic polyurethane derived from polyphenols with different substituent groups, J. Appl. Polym. Sci. 136 (2019) 1–7. https://doi.org/10.1002/app.47039.

[38] S. Xu, D. Sheng, X. Liu, F. Ji, Y. Zhou, L. Dong, H. Wu, Y. Yang, A seawater-assisted self-healing metal–catechol polyurethane with tunable mechanical properties, Polym. Int. 68 (2019) 1084–1090. https://doi.org/10.1002/pi.5798.

[39] J.H. Cho, V. Vasagar, K. Shanmuganathan, A.R. Jones, S. Nazarenko, C.J. Ellison, Bioinspired catecholic flame retardant nanocoating for flexible polyurethane foams, Chem. Mater. 27 (2015) 6784–6790. https://doi.org/10.1021/acs.chemmater.5b03013.

[40] H. Lee, S.M. Dellatore, W.M. Miller, Phillip B. Messersmith, Mussel-inspired surface chemistry for multifunctional coatings, Science. 318 (2007) 426–431. https://doi.org/10.1017/CBO9781107415324.004.

[41] M.J. Sever, J.T. Weisser, J. Monahan, S. Srinivasan, J.J. Wilker, Metal-mediated cross-linking in the generation of a marine-mussel adhesive, Angew. Chem. Int. Ed. 43 (2004) 448–450. https://doi.org/10.1002/anie.200352759.

509 [42] H. Yamamoto, Y. Sakai, K. Ohkawa, Synthesis and wettability characteristics of model
510 adhesive protein sequences inspired by a marine mussel., Biomacromolecules. 1 (2000) 543–551.
511 https://doi.org/10.1021/bm000061p.
512 [43] M. Yu, J. Hwang, T.J. Deming, Role of 1-3,4-dihydroxyphenylalanine in mussel adhesive
513 proteins, J. Am. Chem. Soc. 121 (1999) 5825–5826. https://doi.org/10.1021/ja990469y.
514 [44] M. Yu, T.J. Deming, Synthetic polypeptide mimics of marine adhesives, Macromolecules. 31
515 (1998) 4739–4745. https://doi.org/10.1021/ma980268z.
516 [45] P. Sun, H. Lu, X. Yao, X. Tu, Z. Zheng, X. Wang, Facile and universal immobilization of l-
517 lysine inspired by mussels, J. Mater. Chem. 22 (2012) 10035–10041.
518 https://doi.org/10.1039/c2jm16598h.
519 [46] K. Lei, Y. Sun, C. Sun, D. Zhu, Z. Zheng, X. Wang, Fabrication of a controlled in situ
520 forming polypeptide hydrogel with a good biological compatibility and shapeable property, ACS
521 Appl. Bio Mater. 2 (2019) 1751–1761. https://doi.org/10.1021/acsabm.9b00157.
522 [47] P. Sun, J. Wang, X. Yao, Y. Peng, X. Tu, P. Du, Z. Zheng, X. Wang, Facile preparation of
523 mussel-inspired polyurethane hydrogel and its rapid curing behavior, ACS Appl. Mater. Interfaces.
524 6 (2014) 12495–12504. https://doi.org/10.1021/am502106e.
525 [48] J. Saiz-Poseu, J. Mancebo-Aracil, F. Nador, F. Busqué, D. Ruiz-Molina, The chemistry
526 behind catechol-based adhesion, Angew. Chem. Int. Ed. 58 (2019) 696–714.
527 https://doi.org/10.1002/anie.201801063.
528 [49] D. Taylor, N. O'Mara, E. Ryan, M. Takaza, C. Simms, The fracture toughness of soft tissues,
529 J. Mech. Behav. Biomed. Mater. 6 (2012) 139–147. https://doi.org/10.1016/j.jmbbm.2011.09.018.